Impact of water models on structure and dynamics of ligand-transport tunnels in enzymes derived from molecular dynamics simulations

Nikhil Agrawal[1,2,3], Jan Brezovsky[1,2]*

[1] Laboratory of Biomolecular Interactions and Transport, Department of Gene Expression, Institute of Molecular Biology and Biotechnology, Faculty of Biology, Adam Mickiewicz University, Poznan, Poland

[2] International Institute of Molecular and Cell Biology in Warsaw, Warsaw, Poland

[3] Latvian Institute of Organic Synthesis, Riga, Latvia

Corresponding author: Jan Brezovsky, E-mail: janbre@amu.edu.pl , jbrezovsky@iimcb.gov.pl

ABSTRACT

Protein hydration plays a vital role in many biological functions. Molecular simulations are frequently used to study the effect of hydration on proteins at the atomic level. However, the accuracy of these simulations has often been highly sensitive to the water model used, perhaps best known in the case of intrinsically disordered proteins. In the present study, we have investigated to what extent the choice of a water model alters the behavior of complex networks of transport tunnels, which are critical for function of many enzymes with buried active sites. By performing all-atom molecular dynamics simulations of the haloalkane dehalogenase LinBWT and its two variants, LinB32 and LinB86, with synthetically engineered tunnel networks in TIP3P and OPC water models, we investigated their effects on the overall tunnel topology, properties of the main tunnels such as their conformation, residue composition, and duration of their open states. Our data showed that while all three proteins exhibited similar conformational behavior in both water models, they differed in the duration of openings of their main tunnels and, in limited cases, also in the properties of their auxiliary tunnels. Interestingly, the results indicate that the stability of the open tunnels is sensitive to the water model, rendering the generally more accurate OPC water model a preferred choice here, particularly when the kinetics of the ligand transport process is under question. However, since the TIP3P model can provide comparable inference on the overall topology of the networks of primary tunnels and their geometry, it may still be a relevant option when computational resources are limited.

Keywords: Water models, ligand transport, tunnels, channels, enzymes, MD simulations

INTRODUCTION

Water is indispensable in determining the structure, stability, dynamics, and function of proteins.[1] Water moleuculs plays a critical role in various biological processes such as protein folding and enzymatic catalysis.[2,3] Interfacial/bound and internal/buried water molecules could affect protein-protein association, protein-ligand interaction,[4,5] protein thermal stability, and peptide binding affinity.[6,7] On the other hand, proteins also perturb the dynamics of water molecules. The surface of proteins is highly heterogeneous due to geometrical disorder and the different energetics of the local H-bonds between water and protein sites,[8,9] which can lead to increased residence times of some water molecules in the vicinity of proteins surfaces. It has been estimated that the residence time of such dampened water molecules near the protein surface could be in the range of nanoseconds to microseconds.[10,11] In contrast, the residence time of water molecules buried inside the protein structure could reach up to milliseconds.[1,12] In addition, the proximity of proteins can also affect the reorientational and translational behavior of water molecules; NMR studies have observed that water reorientation and translation near globular proteins is 3−5 times slower than in bulk.[9,13,14]

All-atom molecular dynamics (MD) simulations have been widely employed to investigate protein-water interactions and have provided insight into water properties and their effects on biomolecules.[15,16] The accuracy of simulations of protein immersed in explicit water molecules depends critically on the choice of the protein force field and water model used.[17–19] There is a large number of water model families, but the most commonly applied models are Single Point Charge (SPC),[20] Transferable Intermolecular Potential (TIP),[21] and Optimal Point Charge (OPC).[22] The SPC family includes three-point charges placed on the nuclei and a single 12-6 LJ term centered on the oxygen atom or hydrogen atoms.[20] The TIP family consists of 3-, 4-, and 5-point water models named as TIP3P, TIP4P, and TIP5P, respectively.[23] Finally, the OPC family includes 3- and 4-point water models OPC3 and OPC.[24] These water models provide a good compromise between accuracy and efficient calculations but are imperfect. For example, the kinetic properties of TIP3P such as self-diffusivity and viscosity, do not agree well with the experimental observations but the thermodynamic properties are considered to be a reasonable approximation.[1,25] Historically, most of these water models have been developed in conjunction with a particular protein force field, such as SPC with GROMOS,[26] TIP3P with AMBER and CHARMM,[27,28] and TIP4P with OPLS force fields.[29] Because of its looser coupling to any specific water models, AMBER force fields have also been shown to work with TIP4P, TIP5P, and OPC water models.[30,31]

To date, many studies have been conducted to investigate discrepancies arising from the use of different explicit water models. For example, Anandakrishnan *et al.* used TIP3P and TIP4P/EW models to investigate the protein folding landscape of the mini-protein CLN025, finding almost order-of-magnitude difference in the models ability to predict the fraction of unfolded states and traced the origin of these differences to the water-water electrostatic interactions.[19] Gupta *et al.* studied temperature dependent glass transition of Trp-cage mini-protein using mTIP3P, TIP4P, and TIP4PEw models and found out that the use of the TIP3P model resulted in decreased number of water molecules packed in the first hydration shell of the Trp-cage surface.[32] Importantly, conformational ensembles of intrinsically disordered proteins simulated with different water models were shown to differ strickingly, often being too compact in comparison to various experimental measurements which could primarily be ascribed to weaker dispersion interactions.[33–37] Considering the impact of models on the binding of water molecules to proteins, Fadda *et al.* performed simulations of the Concanavalin A protein in free and ligand-bound forms in TIP3P, TIP4P, and TIP5P models, showing that the binding energies of the isolated water molecule are highly sensitive to the model.[38] Finally, a study on water diffusion through aquaporin AQP1 by Gonzalez *et al*. contrasted TIP3P, OPC, and TIP4P/2005 models to find out that unlike studied 4-point water models, TIP3P had about three times higher osmotic permeability through the protein than indicated by experimental observations.[39] Overall, these studies have suggested that the accuracy of a simulation, in particular when considering less ordered protein fragments as well as interactions and behavior of water molecules inside the protein body, is often rather sensitive to the water models used, which have been developed initially with relatively stable globular proteins in mind.

From this perspective, it is relevant to consider yet another structural element of proteins with the buried functional site, which is connected to the surrounding solvent through empty spaces known as tunnels.[40,41] Tunnels are often equipped with molecular gates, making them transient, switching between closed and open states.[42] The dynamics and structure of tunnels play a critical role in the entry of substrates into the active site and the release of products from the active site into the bulk solvent.[42,43] Another important role of tunnels is to act as a selectivity filter, allowing only to the cognate molecules of substrates or solvents to enter the active site.[44–46] Interestingly, the sensitivity of the tunnels to solvent composition was demonstrated by Stepankova *et al.*, who showed significantly altered openings of tunnel entrances of three different dehalogenases when exposed to three different aqueous solutions containing water-miscible organic co-solvents.[47] Since the tunnels are critical for enzyme function, can be

rationally engineered to provide improved biocatalysts,[40,43] and represent attractive drug targets,[48] it is critical to understand the role of water models on the nature of the tunnel networks observed in the simulated conformational ensembles.

In the present study, we investigated the effect of two different water models on the structure and dynamics of complex tunnel networks in enzymes. For this purpose, we chose the TIP3P water model because of its widespread use,[49] and the OPC model which is one of the best models for reproducing bulk water properties.[24] As a model system with well-understood and diverse tunnel networks, we have used members of the haloalkane dehalogenase (HLDs) family, LinBWT and its two engineered variants, a single-point mutant LinB32 and a four-point mutant LinB86. Structurally, these enzymes belong to the α/β-hydrolase superfamily, characterized by their main and cap domains, with the buried active site at their interface.[50] HLDs have a long-standing history as a model system for the catalytic action of enzymes with buried active sites due to the wealth of data collected on the transport component of their function,[51] including the identification of rate-determining steps,[43,52,53] numerous crystal structures, and in-depth studies of the effect of mutations in the tunnel networks of these enzymes.[40] The three HLD model systems used here have different networks of primary and auxiliary tunnels. In LinBWT, the main tunnel (P1) is prominently open, but in LinB32 and LinB86 variants, the P1 tunnel is blocked by a Leu177Trp mutation, which hinders substrate and product transport.[43,53] In addition, the introduced Trp177 forms a hydrogen bond to Asp147 which induces the cap domain gate of the P1 tunnel.[52] In LinB86, three additional mutations (Trp140Ala+Phe143Leu+Ile211Leu) were introduced into the auxiliary access tunnel P3, resulting in its activation and increasing the flexibility of the cap domain gate of the P1 tunnel.[43,52] These different tunnel networks allowed us to analyze the extent to which the water model used affects our ability to detect relevant tunnels, their bottleneck dimension, the composition of residues that form them, and the duration for which the tunnels remain open.

METHODS

To study the effect of different water models on tunnel dynamics, we have performed simulations for LinBWT, LinB32, and LinB86 enzymes in TIP3P and OPC water models.

Initial structures of LinBWT (PDB ID: 1MJ5),[54] LinB32 (PDB ID: 4WDQ),[43] and LinB86 (PDB ID: 5LKA)[43] were prepared for simulations as described previously.[43] Initial water molecules around protein structures were placed in three steps. In the first step 3D-RISM theory according to the Placevent algorithm, was used to add initial water molecules to protein

structures.[55,56] In the second step, 3D-RISM predicted water molecules were merged with crystallographic water molecules and in the last step water molecules, which had their oxygens atoms within 2Å of protein atoms, were removed. Truncated octahedral water boxes (TIP3P and OPC) were added to the distance of 10 Å from any atom in the respective systems, and ions (Na^+ and Cl^-) were added to make a final concentration of 0.1 M using the *tleap* module of AMBER 18.[57] Hydrogen mass repartitioning (HMR) was performed using the *parmed* module of AMBER 18 to enable 4 fs timestep.[58]

The systems were energy minimized using with the *pmemd* module of AMBER 18, by 100 steepest descent steps followed by 400 conjugate gradient steps within five rounds of decreasing harmonic restrain as follows 500 kcal mol^{-1} $Å^{-2}$ applied on all heavy atoms of protein and then 500, 125, 25, and 0 kcal mol^{-1} $Å^{-2}$ on backbone atoms only. The equilibration of the systems was performed in four stages. In the first round, 20 ps NVT simulations were performed to gradually heat the systems from 0 K to 200 K, followed by 1 ns NVT simulations to reach the target temperature of 310 K. In these two stages, harmonic restraints of 5.0 kcal mol^{-1} $Å^{-2}$ were applied on the heavy atoms of proteins and the temperature was controlled using a Langevin thermostat,[59] with collision frequency set to 2.0 ps^{-1}. The third stage consisted of 1 ns NPT simulations performed at 310 K using the Langevin thermostat and the constant pressure of 1.0 bar using Monte Carlo barostat while keeping restraints of 5.0 kcal mol^{-1} $Å^{-2}$ on proteins backbone atoms only. The last stage employed the same settings as the third one but without any positional restraints.

Finally, unrestrained NPT simulations were run for all investigated systems for 500 ns, saving the data to trajectories at 10 ps intervals. All simulations employed the SHAKE algorithm[60] to fix bonds containing the hydrogens and periodic boundary conditions. The simulations were performed using the *pmemd.cuda* module of AMBER 18 using ff14SB force field.[61] Three replicated simulations were conducted for LinBWT in TIP3P and OPC water models. In contrast, more simulations were performed to obtain at least two open and two closed forms of LinB32 and LinB86 in TIP3P and OPC water models. The initial 100 ns of simulations were dedicated to water and structural equilibration, leaving 400 ns (40,000 frames) for analyses per replicate.

The dynamic behavior of tunnels was analyzed using CAVER 3.0[62] and the starting point was defined by the center of mass of Trp109, His272, and Asn38. Tunnels were searched in each trajectory snapshot using a probe radius of 0.7 Å, shell radius of 3 Å and shell depth of 4 Å.

All identified tunnels were retained in each snapshot. The hierarchical average-link clustering was employed to cluster the tunnels, keeping only the cheapest tunnel per cluster and frame. To enable the separation of P1a and P1b branches of the main tunnel, the clustering threshold of 3 Å was used for LinBWT except for one simulation of LinBWT in the OPC water model for which a clustering threshold of 2.5 Å was used; for all LinB32 and LinB86 simulations clustering threshold of 4.5 Å was sufficient. A tunnel was considered open if its bottleneck radius was greater or equal to 1.4 Å. Tunnels bottleneck residues were plotted which were present for 30% or above in either TIP3P or OPC simulations. Identification and visualization of tunnels representing the geometric average of tunnel clusters was performed using TransportTools library 0.9.5.[63]

The trajectories were clustered using the ward hierarchical clustering procedure with the TTclust program.[64] Trajectory files with a stride size of 2 frames were used and clustering was performed on residue number 11-295 backbone atoms (N, CA, C). To define the open and closed states of dehalogenases we have used the minimum distance between all heavy atoms of Asp147 and Leu177/Trp177 residues. In our study, we considered the cap domain gate is open if the minimum distance was larger than 4 Å. Root-mean-square deviation (RMSD), the radius of gyration, were calculated for residue number 11-295 backbone atoms (N, CA, C). Residue-wise root mean square fluctuation (RMSF) was calculated using backbone atoms (N, CA, C) of residue 1-295. Radial distribution function (RDF) was calculated for water (O, H1, H2 atoms), around Asp108 (CG atom), with a bin spacing of 0.1 Å, and a maximum bin value of 15 Å. All these analyses were performed using the *cpptraj* module of AMBER 18.[65]

RESULTS AND DISCUSSION

Conformational states of cap domain gaate in dehalogenases are structurally comparable between OPC and TIP3P but their accessibilities may not be

In a previous study, Damborsky *et al.* using experimental and simulation techniques discovered that LinB32 and LinB86 can adopt open and closed conformations due to the marked movement of one of the cap domain helices after the hydrogen bond between the Asp147 and mutated Trp177 is broken.[52] More, these open and closed states were shown to be coupled with very different enzymatic efficiency,[52] and hence should be considered separately. To identify the open and closed states of these proteins in our simulations, we have calculated the percentage of time the gate between resides 147 and 177 remained open for water molecules in each studied system (Table S1). Due to the lack of hydrogen bond stabilizing the closed

conformation of this gate, each of the three initially performed simulations of LinBWT with both water models exhibited almost exclusively open state. In case of mutants, additional simulations had to be run to obtain at least two simulations sufficiently sampling the opened states for at least 20 % of time. For LinB32 with OPC water model, the discovery of open states presented challenge, requiring about twice as many screening simulations as in other simulated systems, which is well in line with slower sampling of the opening process in OPC and previously established enhanced structural stability of the cap-domain helical gate in this mutant.[43,52] The final set of two simulations with the most often open state (LinB32-Open and LinB86-Open) and the two most often closed simulations (LinB32-Closed and LinB86-Closed) were assembled for each water model (Table S1).

The production phases of all selected simulations exhibited a very stable structure with respect to their initial conformations (Figures S1 and S2). The RMSF profiles in all variants were comparable between the two water models, with the most marked difference in short regions formed by residues 150-160 and 210-220 in LinB86-Open systems (Figure S3). To further probe the effect of water models on conformational diversity adopted by investigated enzymes, we clustered the sampled conformations using TTclut. The obtained representative structures exhibited high similarity across all investigated systems (Figure S4), as well as within the systems, illustrated by the average RMSD between the obtained clusters below 1.1 Å (Table S2). Finally, we have evaluated the RDF of water molecules around the CG atom of catalytic residue Asp108, which is conveniently localized at the bottom of the cavity and can serve as an indicator of solvation levels for the investigated transport tunnels (Figure S5). The obtained density data showed a very good resemblance between the simulations in both water models. Overall, these analyses confirmed the absence of major differences between conformations of analyzed dehalogenases and their overall solvation when simulated in TIP3P and OPC, despite the different likelihood of accessing the open states (Table S1).

Openness of main tunnels and their response to tunnel engineering is comparable between OPC and TIP3P

A tunnel works as a dynamic filter that plays an essential role in enzyme activity. The tunnel's opening leads to the entry and exit of the substrate, product, ions, and solvent molecules in or out of the enzymes.[48] To understand the effect of water models on the opening of tunnel network in these enzymes, we have calculated how often the tunnels were opened for a

spherical probe of 1.4 Å radius (Figures S6-S10), focusing our analysis on the tunnels established in dehalogenase family (P1, P2, and P3).[66]

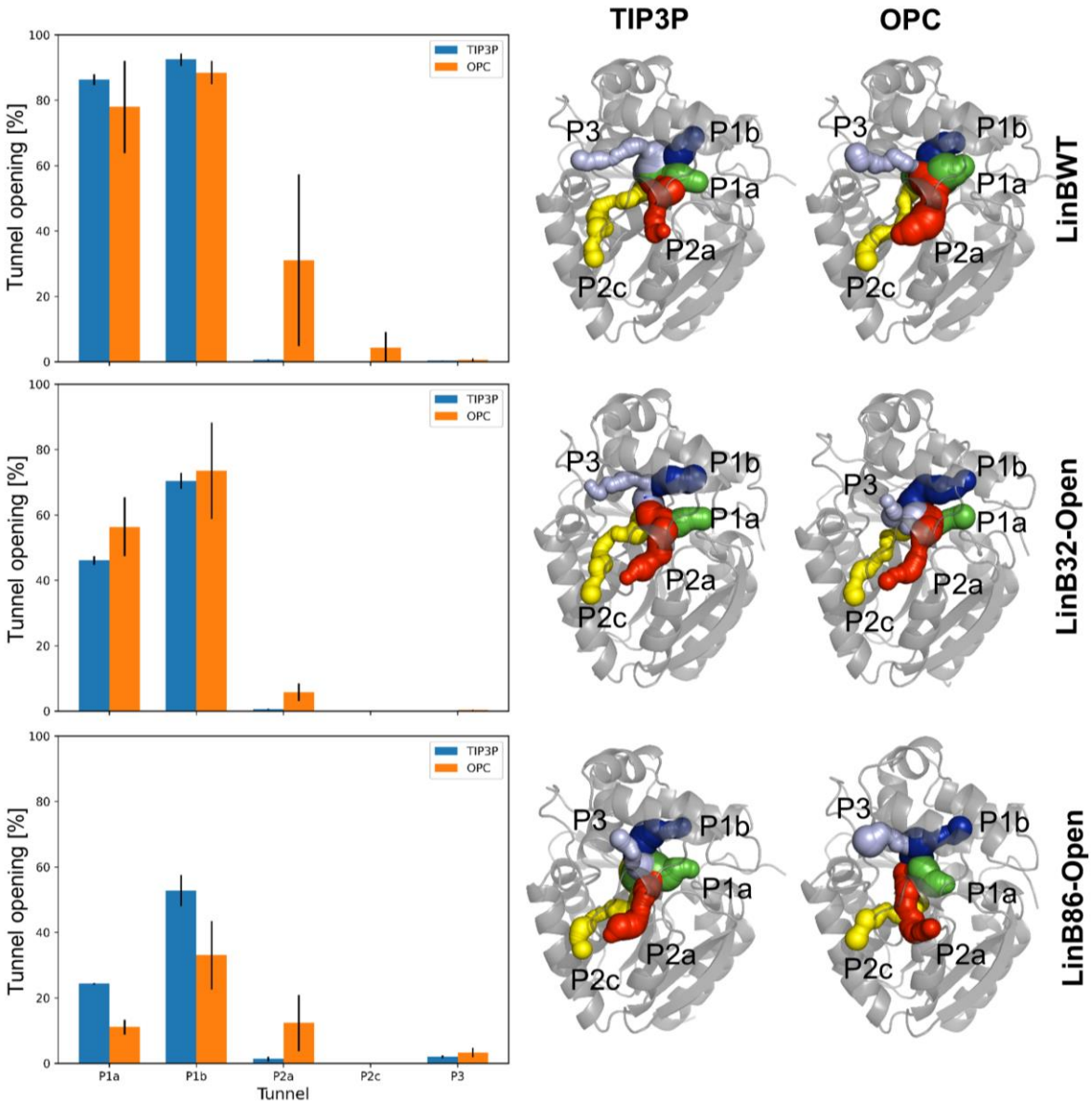

Figure 1 Tunnel network identified in open conformations of studied LinB variants simulated in TIP3P and OPC water models. The availability of tunnels for probe of 1.4 Å in the simulations. The tunnel openness for closed conformations is available in Figure S11. The structure of representative tunnel networks with their bottleneck radius, length, and curvature closest to the average properties of individual tunnel clusters.

In LinBWT, the two branches of its main tunnel (P1a and P1b) remained open for most of the simulation time (Figures 1 and S6) irrespective of the water model used. The most apparent difference in LinBWT simulations was in cases of two branches of auxiliary P2a and P2c, which were observed significantly open in OPC, but negligible in the TIP3P (Figures 1 and S6). In LinB32-Open simulations, the effect of the Leu177Trp mutation on the opening of P1a

and P1b tunnels was consistent between the water models. The availability of the P1a branch was about halved, which agrees with previous simulations performed for this system in TIP3P.[43] We still observed an appreciable opening of the P2a auxiliary tunnel in OPC but not in TIP3P (Figures 1 and S7). In LinB86-Open simulations, the opening was seen in both main (P1a, P1b) and auxiliary tunnels (P2a, P3) in both water models. Again, in line with previous observations,[43] this mutant exhibited a further reduction in main tunnel opennesses and consistent opening of engineered P3 tunnel. In this system, main tunnels showed a more frequent opening in TIP3P, and conversely, opened auxiliary tunnels were more prevalent in OPC (Figures 1 and S8). In the simulations of closed states of both LinB mutants, the branches of the main tunnel were effectively closed in OPC. In contrast, only a minor opening of these branches on the level of auxiliary tunnels was detected in TIP3P (Figures S9-S11). Only the P2a tunnel was consistently open in both water models and represented the primary path available in this closed conformation. Overall, this data suggests that both water models can detect similar tunnel networks with minor differences only and provide comparable inference into the effect of mutations on the tunnels' relevance. This is well in line with the identification of comparable native state of CLN025 mini-protein with different water models but with drastically different proportions of unfolded states.[19] In contrast, the slight preference of OPC simulations for auxiliary tunnels indicates that OPC molecules could more frequently infringe into the protein surface, thereby inducing minor expansions of these tunnels, which is supported by a more tight packing of watere molecules at the the Trp-cage surface, modeled with two different 4-site water models.[32]

Bottleneck dimansion and bottlneck-residues of main tunnels are maintained in both models

Tunnel geometry plays a crucial role in the specificity, activity, and stability of enzymes, in particular the dimension and composition of the bottleneck is critical. This is well illustrated by an example where a single point mutation Y176A was introduced into the bottleneck of main tunnel of DhaA enzyme, markedly opening the tunnel and accelerating the binding of fluorescent probe by three orders of magnitute.[67] Due to the vital role of tunnel bottlenecks, we have investigated the effect of water models on bottleneck geometries and the composition of the defining residues, focusing here on the main tunnel branches (P1a, P1b) that were frequently detected in our simulations to enable their detailed analysis.

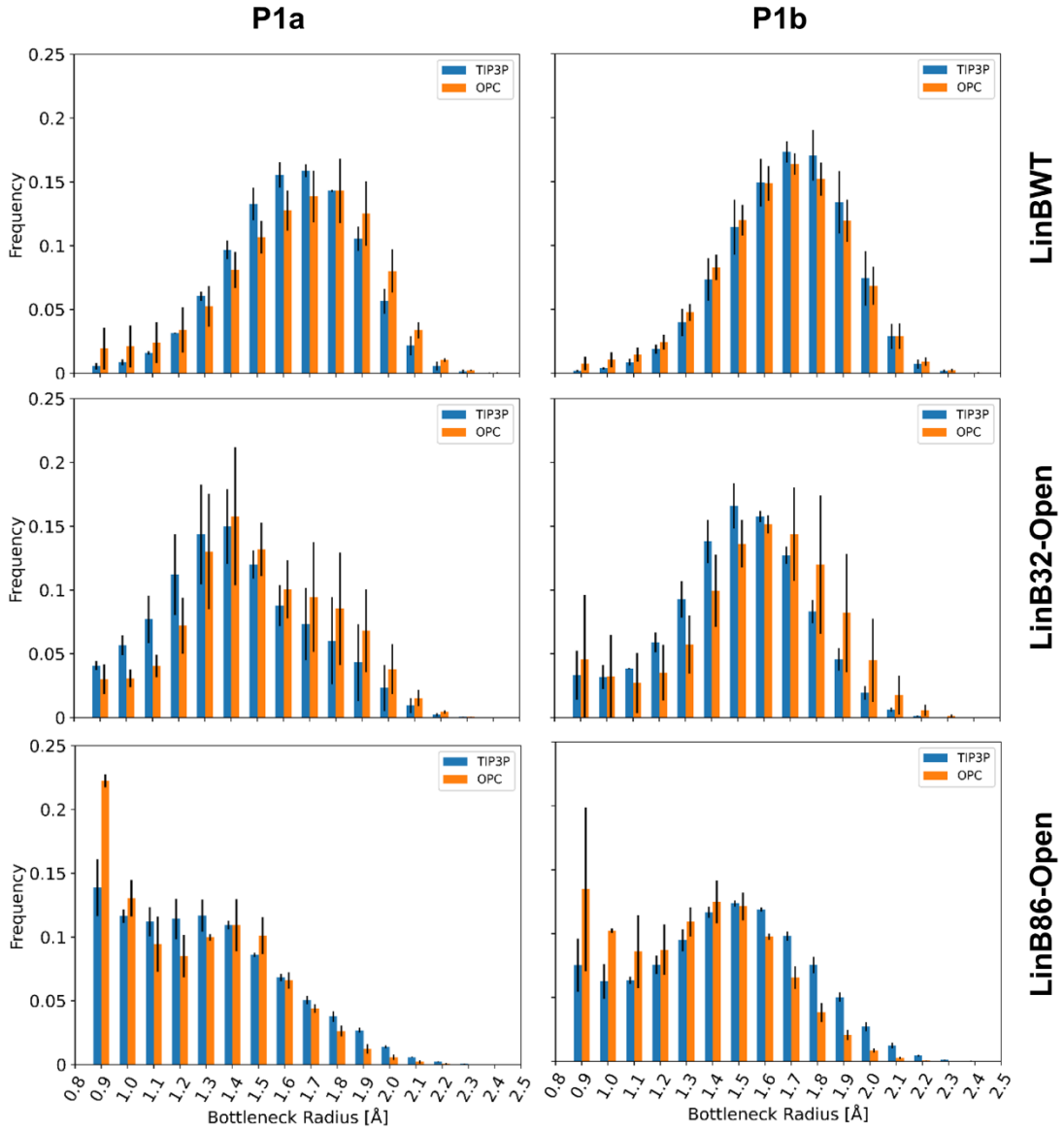

Figure 2 Bottleneck radii distribution in main tunnels P1a and P1b found in studied open conformations of LinB variants simulated in TIP3P and OPC water models.

LinBWT data for tunnel geometries revealed that the geometries of main tunnels in both water models were qualitatively similar. We could detect some relevant differences in bottleneck radii of open P1a tunnels. In TIP3P, these tunnels were more likely to have radii within the 1.4-1.7 Å range, while in OPC, these tunnels more often opened above 1.9 Å (Figure 2). Similarly, the overall trends in the frequency of tunnel geometries in both water models were comparable in LinB32-Open simulations, with a small tendency of both P1a and P1b tunnels towards higher openness in simulations employing OPC (Figure 2). In LinB86-Open simulations, the main tunnels again showed similar profiles. However, in this system, we could observe the opposite trend, in which simulations in OPC more often resulted in narrower tunnels with ~0.9 Å radius and less often produced more widely open tunnels (Figure 2).

Considering the major contributing residues defining the bottleneck regions of P1a and P1b tunnels throughout the simulations, we observed reasonable agreement between OPC- and TIP3P-generated ensembles (Figure S12). Here, the most deviating presence for bottleneck residues was identified for residues that less frequently contributed to the bottleneck formation in the first place (around 50 % in at least one of the datasets), diminishing the potential impact of those differences on the inference of the key residues. In summary, these results indicate that the radii and the residue composition of critical tunnel bottlenecks of the primary tunnels were reasonably well maintained in simulations with either of the two evaluated water models.

Opening states of main tunnels are maintained longer in OPC than in TIP3P

To understand the effect of water models on the stability of the functionally relevant open state of tunnels, we have monitored the duration of the open state of the main tunnels before they undergo a closing process (Figure 3). Unsurprisingly, the large majority of the opening events in the main tunnels were concluded in timescales between 10-100 ps in all simulated systems. However, we have sporadically observed openings with duration between 1-8 ns. Tunnel opening data for LinBWT protein revealed that the opening stability of both main tunnels was similar in both water models. The most distinct difference for this system could be observed for the long-tailed events in the P1b tunnel, where the most prolonged period of opened state was about 5 and 7 ns in TIP3P and OPC, respectively. In the LinB32-Open simulations, we observed a marked increase in the duration of tunnel openings in OPC water models, which was far more pronounced for the P1b tunnel, reaching ~ 1.5 ns in TIP3P and up to 6 ns in OPC. This observation is supported by the overestimated permeability of TIP3P water molecules seen in aquaporin AQP1[39] and the underestimated binding affinity of these molecules in the interior of the Concanavalin A protein,[38] which could diminish their contribution to stabilization of the open state. Similarly to the situation in LinBWT, the differences in the tunnels' opening duration in LinB86-Open were comparable between the two models, including the stabilities of the longest open tunnels reaching up to about 1.5-2.0 ns. To sum up, the water models can markedly affect the stabilization of the open tunnel states, which can have severe implications for the effectiveness of their ability to transport small molecules. However, this observation is system specific and seems more pronounced in the least accessible LinB32 protein. In contrast, the differences in LinBWT with native open tunnels as well as in LinB86 with extra tunnel and enhanced dynamics of cap domain gate were much less accentuated.

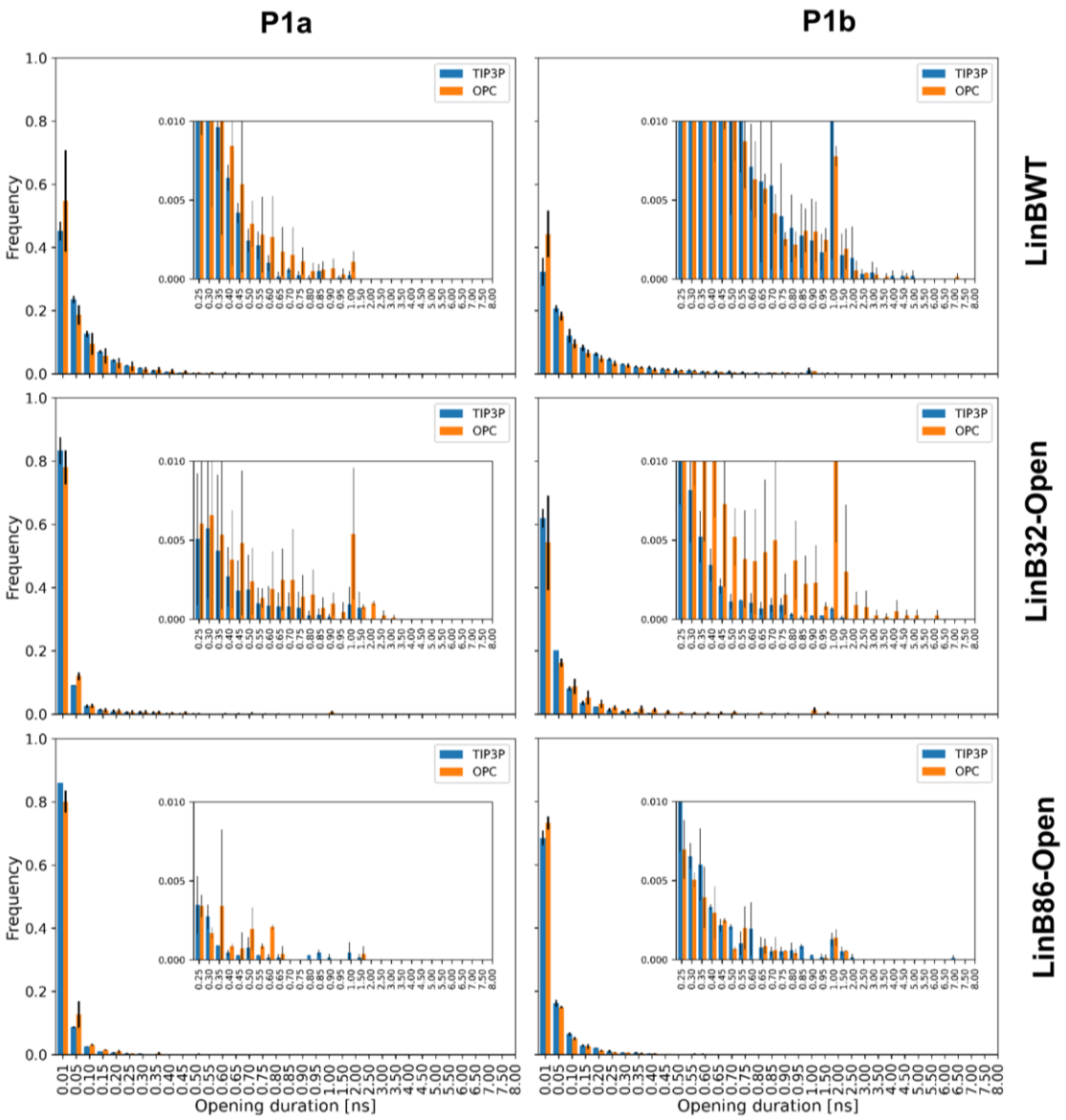

Figure 3 Duration of open states of main tunnels P1a and P1b found in studied open conformations of LinB variants simulated in TIP3P and OPC water models. The insets show less frequent openings with the duration over 0.25 ns.

CONCLUSION

We have performed a series of MD simulations of LinBWT and its two engineered variants in TIP3P and OPC water models. Our simulations showed that structurally proteins behaved very similarly in both water models exploring almost identical conformations which resulted in the detection of similar networks of transport tunnels. With these proteins, the OPC model simulations indicated increased success in identifying narrower auxiliary tunnels over TIP3P simulations. However, we have observed marked sensitivity of the stability of open states to the water model used, making their choice important when ligand (un)binding kinetics is of

interest, e.g., when estimating residence times of inhibitors within the drug discovery frameworks.[68–70] Given the overestimated diffusivity of bulk TIP3P and its unrealistic migration rates via aquaporin AQP1, we believe the OPC water model represents a better choice under these circumstances. Nonetheless, considering the aforementioned points, we suggest that the 3-point TIP3P model could still be of use for the investigation of network topology and geometry in scenarios where available computational resources may prohibit the use of the more costly 4-point OPC model.

Acknowledgments

This work was supported by the National Science Centre, Poland (grant no. 2017/26/E/NZ1/00548). N.A. acknowledges the ERDF postdoc grant (no. 1.1.1.2/VIAA/4/20/757) for financial support. The computations were performed at the Poznan Supercomputing and Networking Center. The authors are grateful to Bartłomiej Surpeta and Carlos Sequeiros-Borja for critical reading of the manuscript.

Authors contributions

N.A. performed all calculations, analyzed data, and co-written the manuscript; J.B. conceived the project, designed the calculation, analyzed data, and co-written the manuscript.

REFERENCES

(1) Bellissent-Funel, M.-C.; Hassanali, A.; Havenith, M.; Henchman, R.; Pohl, P.; Sterpone, F.; van der Spoel, D.; Xu, Y.; Garcia, A. E. Water Determines the Structure and Dynamics of Proteins. *Chem. Rev.* **2016**, *116* (13), 7673–7697. https://doi.org/10.1021/acs.chemrev.5b00664.

(2) Frauenfelder, H.; Fenimore, P. W.; Chen, G.; McMahon, B. H. Protein Folding Is Slaved to Solvent Motions. *Proc. Natl. Acad. Sci.* **2006**, *103* (42), 15469–15472. https://doi.org/10.1073/pnas.0607168103.

(3) Mallamace, F.; Corsaro, C.; Mallamace, D.; Vasi, S.; Vasi, C.; Dugo, G. The Role of Water in Protein's Behavior: The Two Dynamical Crossovers Studied by NMR and FTIR Techniques. *Comput. Struct. Biotechnol. J.* **2015**, *13*, 33–37. https://doi.org/10.1016/j.csbj.2014.11.007.

(4) Ahmed, M. H.; Spyrakis, F.; Cozzini, P.; Tripathi, P. K.; Mozzarelli, A.; Scarsdale, J. N.; Safo, M. A.; Kellogg, G. E. Bound Water at Protein-Protein Interfaces: Partners, Roles and Hydrophobic Bubbles as a Conserved Motif. *PLoS ONE* **2011**, *6* (9), e24712. https://doi.org/10.1371/journal.pone.0024712.

(5) Schiebel, J.; Gaspari, R.; Wulsdorf, T.; Ngo, K.; Sohn, C.; Schrader, T. E.; Cavalli, A.; Ostermann, A.; Heine, A.; Klebe, G. Intriguing Role of Water in Protein-Ligand Binding Studied by Neutron Crystallography on Trypsin Complexes. *Nat. Commun.* **2018**, *9* (1), 3559. https://doi.org/10.1038/s41467-018-05769-2.

(6) Rahaman, O.; Kalimeri, M.; Melchionna, S.; Hénin, J.; Sterpone, F. Role of Internal Water on Protein Thermal Stability: The Case of Homologous G Domains. *J. Phys. Chem. B* **2015**, *119* (29), 8939–8949. https://doi.org/10.1021/jp507571u.

(7) Petrone, P. M.; Garcia, A. E. MHC-Peptide Binding Is Assisted by Bound Water Molecules. *J. Mol. Biol.* **2004**, *338* (2), 419–435. https://doi.org/10.1016/j.jmb.2004.02.039.
(8) Grossman, M.; Born, B.; Heyden, M.; Tworowski, D.; Fields, G. B.; Sagi, I.; Havenith, M. Correlated Structural Kinetics and Retarded Solvent Dynamics at the Metalloprotease Active Site. *Nat. Struct. Mol. Biol.* **2011**, *18* (10), 1102–1108. https://doi.org/10.1038/nsmb.2120.
(9) Grebenkov, D. S.; Goddard, Y. A.; Diakova, G.; Korb, J.-P.; Bryant, R. G. Dimensionality of Diffusive Exploration at the Protein Interface in Solution. *J. Phys. Chem. B* **2009**, *113* (40), 13347–13356. https://doi.org/10.1021/jp9048082.
(10) Persson, F.; Söderhjelm, P.; Halle, B. How Proteins Modify Water Dynamics. *J. Chem. Phys.* **2018**, *148* (21), 215103. https://doi.org/10.1063/1.5026861.
(11) Barnes, R.; Sun, S.; Fichou, Y.; Dahlquist, F. W.; Heyden, M.; Han, S. Spatially Heterogeneous Surface Water Diffusivity around Structured Protein Surfaces at Equilibrium. *J. Am. Chem. Soc.* **2017**, *139* (49), 17890–17901. https://doi.org/10.1021/jacs.7b08606.
(12) Denisov, V. P.; Peters, J.; Hörlein, H. D.; Halle, B. Using Buried Water Molecules to Explore the Energy Landscape of Proteins. *Nat. Struct. Biol.* **1996**, *3* (6), 505–509. https://doi.org/10.1038/nsb0696-505.
(13) Halle, B. Protein Hydration Dynamics in Solution: A Critical Survey. *Philos. Trans. R. Soc. Lond. B. Biol. Sci.* **2004**, *359* (1448), 1207–1223; discussion 1223-1224, 1323–1328. https://doi.org/10.1098/rstb.2004.1499.
(14) Mukherjee, S.; Mondal, S.; Bagchi, B. Distinguishing Dynamical Features of Water inside Protein Hydration Layer: Distribution Reveals What Is Hidden behind the Average. *J. Chem. Phys.* **2017**, *147* (2), 024901. https://doi.org/10.1063/1.4990693.
(15) Copie, G.; Cleri, F.; Blossey, R.; Lensink, M. F. On the Ability of Molecular Dynamics Simulation and Continuum Electrostatics to Treat Interfacial Water Molecules in Protein-Protein Complexes. *Sci. Rep.* **2016**, *6* (1), 38259. https://doi.org/10.1038/srep38259.
(16) Hollingsworth, S. A.; Dror, R. O. Molecular Dynamics Simulation for All. *Neuron* **2018**, *99* (6), 1129–1143. https://doi.org/10.1016/j.neuron.2018.08.011.
(17) Wang, A.; Zhang, Z.; Li, G. Higher Accuracy Achieved in the Simulations of Protein Structure Refinement, Protein Folding, and Intrinsically Disordered Proteins Using Polarizable Force Fields. *J. Phys. Chem. Lett.* **2018**, *9* (24), 7110–7116. https://doi.org/10.1021/acs.jpclett.8b03471.
(18) Piana, S.; Donchev, A. G.; Robustelli, P.; Shaw, D. E. Water Dispersion Interactions Strongly Influence Simulated Structural Properties of Disordered Protein States. *J. Phys. Chem. B* **2015**, *119* (16), 5113–5123. https://doi.org/10.1021/jp508971m.
(19) Anandakrishnan, R.; Izadi, S.; Onufriev, A. V. Why Computed Protein Folding Landscapes Are Sensitive to the Water Model. *J. Chem. Theory Comput.* **2019**, *15* (1), 625–636. https://doi.org/10.1021/acs.jctc.8b00485.
(20) Glättli, A.; Daura, X.; van Gunsteren, W. F. Derivation of an Improved Simple Point Charge Model for Liquid Water: SPC/A and SPC/L. *J. Chem. Phys.* **2002**, *116* (22), 9811–9828. https://doi.org/10.1063/1.1476316.
(21) Jorgensen, W. L. Quantum and Statistical Mechanical Studies of Liquids. 10. Transferable Intermolecular Potential Functions for Water, Alcohols, and Ethers. Application to Liquid Water. *J. Am. Chem. Soc.* **1981**, *103* (2), 335–340. https://doi.org/10.1021/ja00392a016.
(22) Izadi, S.; Anandakrishnan, R.; Onufriev, A. V. Building Water Models: A Different Approach. *J. Phys. Chem. Lett.* **2014**, *5* (21), 3863–3871. https://doi.org/10.1021/jz501780a.
(23) Harrach, M. F.; Drossel, B. Structure and Dynamics of TIP3P, TIP4P, and TIP5P Water near Smooth and Atomistic Walls of Different Hydroaffinity. *J. Chem. Phys.* **2014**, *140* (17), 174501. https://doi.org/10.1063/1.4872239.
(24) Xiong, Y.; Shabane, P. S.; Onufriev, A. V. Melting Points of OPC and OPC3 Water Models. *ACS Omega* **2020**, *5* (39), 25087–25094. https://doi.org/10.1021/acsomega.0c02638.
(25) Onufriev, A. V.; Izadi, S. Water Models for Biomolecular Simulations. *WIREs Comput. Mol. Sci.* **2018**, *8* (2), e1347. https://doi.org/10.1002/wcms.1347.

(26) Oostenbrink, C.; Villa, A.; Mark, A. E.; Van Gunsteren, W. F. A Biomolecular Force Field Based on the Free Enthalpy of Hydration and Solvation: The GROMOS Force-Field Parameter Sets 53A5 and 53A6. *J. Comput. Chem.* **2004**, *25* (13), 1656–1676. https://doi.org/10.1002/jcc.20090.
(27) Cornell, W. D.; Cieplak, P.; Bayly, C. I.; Gould, I. R.; Merz, K. M.; Ferguson, D. M.; Spellmeyer, D. C.; Fox, T.; Caldwell, J. W.; Kollman, P. A. A Second Generation Force Field for the Simulation of Proteins, Nucleic Acids, and Organic Molecules. *J. Am. Chem. Soc.* **1995**, *117* (19), 5179–5197. https://doi.org/10.1021/ja00124a002.
(28) Boonstra, S.; Onck, P. R.; van der Giessen, E. CHARMM TIP3P Water Model Suppresses Peptide Folding by Solvating the Unfolded State. *J. Phys. Chem. B* **2016**, *120* (15), 3692–3698. https://doi.org/10.1021/acs.jpcb.6b01316.
(29) Jorgensen, W. L.; Tirado-Rives, J. The OPLS [Optimized Potentials for Liquid Simulations] Potential Functions for Proteins, Energy Minimizations for Crystals of Cyclic Peptides and Crambin. *J. Am. Chem. Soc.* **1988**, *110* (6), 1657–1666. https://doi.org/10.1021/ja00214a001.
(30) Zhang, H.; Yin, C.; Jiang, Y.; van der Spoel, D. Force Field Benchmark of Amino Acids: I. Hydration and Diffusion in Different Water Models. *J. Chem. Inf. Model.* **2018**, *58* (5), 1037–1052. https://doi.org/10.1021/acs.jcim.8b00026.
(31) Shabane, P. S.; Izadi, S.; Onufriev, A. V. General Purpose Water Model Can Improve Atomistic Simulations of Intrinsically Disordered Proteins. *J. Chem. Theory Comput.* **2019**, *15* (4), 2620–2634. https://doi.org/10.1021/acs.jctc.8b01123.
(32) Gupta, M.; Chakravarty, C.; Bandyopadhyay, S. Sensitivity of Protein Glass Transition to the Choice of Water Model. *J. Chem. Theory Comput.* **2016**, *12* (11), 5643–5655. https://doi.org/10.1021/acs.jctc.6b00825.
(33) Nerenberg, P. S.; Head-Gordon, T. Optimizing Protein−Solvent Force Fields to Reproduce Intrinsic Conformational Preferences of Model Peptides. *J. Chem. Theory Comput.* **2011**, *7* (4), 1220–1230. https://doi.org/10.1021/ct2000183.
(34) Piana, S.; Donchev, A. G.; Robustelli, P.; Shaw, D. E. Water Dispersion Interactions Strongly Influence Simulated Structural Properties of Disordered Protein States. *J. Phys. Chem. B* **2015**, *119* (16), 5113–5123. https://doi.org/10.1021/jp508971m.
(35) Best, R. B.; Zheng, W.; Mittal, J. Balanced Protein-Water Interactions Improve Properties of Disordered Proteins and Non-Specific Protein Association. *J. Chem. Theory Comput.* **2014**, *10* (11), 5113–5124. https://doi.org/10.1021/ct500569b.
(36) Huang, J.; Rauscher, S.; Nawrocki, G.; Ran, T.; Feig, M.; de Groot, B. L.; Grubmüller, H.; MacKerell, A. D. CHARMM36m: An Improved Force Field for Folded and Intrinsically Disordered Proteins. *Nat. Methods* **2017**, *14* (1), 71–73. https://doi.org/10.1038/nmeth.4067.
(37) Rauscher, S.; Gapsys, V.; Gajda, M. J.; Zweckstetter, M.; de Groot, B. L.; Grubmüller, H. Structural Ensembles of Intrinsically Disordered Proteins Depend Strongly on Force Field: A Comparison to Experiment. *J. Chem. Theory Comput.* **2015**, *11* (11), 5513–5524. https://doi.org/10.1021/acs.jctc.5b00736.
(38) Fadda, E.; Woods, R. J. On the Role of Water Models in Quantifying the Binding Free Energy of Highly Conserved Water Molecules in Proteins: The Case of Concanavalin A. *J. Chem. Theory Comput.* **2011**, *7* (10), 3391–3398. https://doi.org/10.1021/ct200404z.
(39) Gonzalez, M. A.; Zaragoza, A.; Lynch, C. I.; Sansom, M. S. P.; Valeriani, C. Influence of Water Models on Water Movement through AQP1. *J. Chem. Phys.* **2021**, *155* (15), 154502. https://doi.org/10.1063/5.0063986.
(40) Kokkonen, P.; Bednar, D.; Pinto, G.; Prokop, Z.; Damborsky, J. Engineering Enzyme Access Tunnels. *Biotechnol. Adv.* **2019**, *37* (6), 107386. https://doi.org/10.1016/j.biotechadv.2019.04.008.
(41) Kingsley, L. J.; Lill, M. A. Substrate Tunnels in Enzymes: Structure–Function Relationships and Computational Methodology. *Proteins Struct. Funct. Bioinforma.* **2015**, *83* (4), 599–611. https://doi.org/10.1002/prot.24772.

(42) Gora, A.; Brezovsky, J.; Damborsky, J. Gates of Enzymes. *Chem. Rev.* **2013**, *113* (8), 5871–5923. https://doi.org/10.1021/cr300384w.
(43) Brezovsky, J.; Babkova, P.; Degtjarik, O.; Fortova, A.; Gora, A.; Iermak, I.; Rezacova, P.; Dvorak, P.; Smatanova, I. K.; Prokop, Z.; Chaloupkova, R.; Damborsky, J. Engineering a de Novo Transport Tunnel. *ACS Catal.* **2016**, *6* (11), 7597–7610. https://doi.org/10.1021/acscatal.6b02081.
(44) Zhou, H.-X.; Wlodek, S. T.; McCammon, J. A. Conformation Gating as a Mechanism for Enzyme Specificity. *Proc. Natl. Acad. Sci.* **1998**, *95* (16), 9280–9283. https://doi.org/10.1073/pnas.95.16.9280.
(45) Liebgott, P.-P.; Leroux, F.; Burlat, B.; Dementin, S.; Baffert, C.; Lautier, T.; Fourmond, V.; Ceccaldi, P.; Cavazza, C.; Meynial-Salles, I.; Soucaille, P.; Fontecilla-Camps, J. C.; Guigliarelli, B.; Bertrand, P.; Rousset, M.; Léger, C. Relating Diffusion along the Substrate Tunnel and Oxygen Sensitivity in Hydrogenase. *Nat. Chem. Biol.* **2010**, *6* (1), 63–70. https://doi.org/10.1038/nchembio.276.
(46) Koudelakova, T.; Chaloupkova, R.; Brezovsky, J.; Prokop, Z.; Sebestova, E.; Hesseler, M.; Khabiri, M.; Plevaka, M.; Kulik, D.; Kuta Smatanova, I.; Rezacova, P.; Ettrich, R.; Bornscheuer, U. T.; Damborsky, J. Engineering Enzyme Stability and Resistance to an Organic Cosolvent by Modification of Residues in the Access Tunnel. *Angew. Chem. Int. Ed.* **2013**, *52* (7), 1959–1963. https://doi.org/10.1002/anie.201206708.
(47) Stepankova, V.; Khabiri, M.; Brezovsky, J.; Pavelka, A.; Sykora, J.; Amaro, M.; Minofar, B.; Prokop, Z.; Hof, M.; Ettrich, R.; Chaloupkova, R.; Damborsky, J. Expansion of Access Tunnels and Active-Site Cavities Influence Activity of Haloalkane Dehalogenases in Organic Cosolvents. *ChemBioChem* **2013**, *14* (7), 890–897. https://doi.org/10.1002/cbic.201200733.
(48) Marques, S. M.; Daniel, L.; Buryska, T.; Prokop, Z.; Brezovsky, J.; Damborsky, J. Enzyme Tunnels and Gates As Relevant Targets in Drug Design. *Med. Res. Rev.* **2017**, *37* (5), 1095–1139. https://doi.org/10.1002/med.21430.
(49) Emperador, A.; Crehuet, R.; Guàrdia, E. Effect of the Water Model in Simulations of Protein-Protein Recognition and Association. *Polymers* **2021**, *13* (2), 176. https://doi.org/10.3390/polym13020176.
(50) Bauer, T. L.; Buchholz, P. C. F.; Pleiss, J. The Modular Structure of α/β-Hydrolases. *FEBS J.* **2020**, *287* (5), 1035–1053. https://doi.org/10.1111/febs.15071.
(51) Chaloupková, R.; Sýkorová, J.; Prokop, Z.; Jesenská, A.; Monincová, M.; Pavlová, M.; Tsuda, M.; Nagata, Y.; Damborský, J. Modification of Activity and Specificity of Haloalkane Dehalogenase from Sphingomonas Paucimobilis UT26 by Engineering of Its Entrance Tunnel*. *J. Biol. Chem.* **2003**, *278* (52), 52622–52628. https://doi.org/10.1074/jbc.M306762200.
(52) Kokkonen, P.; Sykora, J.; Prokop, Z.; Ghose, A.; Bednar, D.; Amaro, M.; Beerens, K.; Bidmanova, S.; Slanska, M.; Brezovsky, J.; Damborsky, J.; Hof, M. Molecular Gating of an Engineered Enzyme Captured in Real Time. *J. Am. Chem. Soc.* **2018**, *140* (51), 17999–18008. https://doi.org/10.1021/jacs.8b09848.
(53) Biedermannová, L.; Prokop, Z.; Gora, A.; Chovancová, E.; Kovács, M.; Damborský, J.; Wade, R. C. A Single Mutation in a Tunnel to the Active Site Changes the Mechanism and Kinetics of Product Release in Haloalkane Dehalogenase LinB*. *J. Biol. Chem.* **2012**, *287* (34), 29062–29074. https://doi.org/10.1074/jbc.M112.377853.
(54) Oakley, A. J.; Klvaňa, M.; Otyepka, M.; Nagata, Y.; Wilce, M. C. J.; Damborský, J. Crystal Structure of Haloalkane Dehalogenase LinB from Sphingomonas Paucimobilis UT26 at 0.95 Å Resolution: Dynamics of Catalytic Residues,. *Biochemistry* **2004**, *43* (4), 870–878. https://doi.org/10.1021/bi034748g.
(55) Sindhikara, D. J.; Hirata, F. Analysis of Biomolecular Solvation Sites by 3D-RISM Theory. *J. Phys. Chem. B* **2013**, *117* (22), 6718–6723. https://doi.org/10.1021/jp4046116.
(56) Sindhikara, D. J.; Yoshida, N.; Hirata, F. Placevent: An Algorithm for Prediction of Explicit Solvent Atom Distribution—Application to HIV-1 Protease and F-ATP Synthase. *J. Comput. Chem.* **2012**, *33* (18), 1536–1543. https://doi.org/10.1002/jcc.22984.

(57) Lee, T.-S.; Cerutti, D. S.; Mermelstein, D.; Lin, C.; LeGrand, S.; Giese, T. J.; Roitberg, A.; Case, D. A.; Walker, R. C.; York, D. M. GPU-Accelerated Molecular Dynamics and Free Energy Methods in Amber18: Performance Enhancements and New Features. *J. Chem. Inf. Model.* **2018**, *58* (10), 2043–2050. https://doi.org/10.1021/acs.jcim.8b00462.
(58) Hopkins, C. W.; Le Grand, S.; Walker, R. C.; Roitberg, A. E. Long-Time-Step Molecular Dynamics through Hydrogen Mass Repartitioning. *J. Chem. Theory Comput.* **2015**, *11* (4), 1864–1874. https://doi.org/10.1021/ct5010406.
(59) Zwanzig, R. Nonlinear Generalized Langevin Equations. *J. Stat. Phys.* **1973**, *9* (3), 215–220. https://doi.org/10.1007/BF01008729.
(60) Ryckaert, J.-P.; Ciccotti, G.; Berendsen, H. J. C. Numerical Integration of the Cartesian Equations of Motion of a System with Constraints: Molecular Dynamics of n-Alkanes. *J. Comput. Phys.* **1977**, *23* (3), 327–341. https://doi.org/10.1016/0021-9991(77)90098-5.
(61) Maier, J. A.; Martinez, C.; Kasavajhala, K.; Wickstrom, L.; Hauser, K. E.; Simmerling, C. Ff14SB: Improving the Accuracy of Protein Side Chain and Backbone Parameters from Ff99SB. *J. Chem. Theory Comput.* **2015**, *11* (8), 3696–3713. https://doi.org/10.1021/acs.jctc.5b00255.
(62) Chovancova, E.; Pavelka, A.; Benes, P.; Strnad, O.; Brezovsky, J.; Kozlikova, B.; Gora, A.; Sustr, V.; Klvana, M.; Medek, P.; Biedermannova, L.; Sochor, J.; Damborsky, J. CAVER 3.0: A Tool for the Analysis of Transport Pathways in Dynamic Protein Structures. *PLOS Comput. Biol.* **2012**, *8* (10), e1002708. https://doi.org/10.1371/journal.pcbi.1002708.
(63) Brezovsky, J.; Thirunavukarasu, A. S.; Surpeta, B.; Sequeiros-Borja, C. E.; Mandal, N.; Sarkar, D. K.; Dongmo Foumthuim, C. J.; Agrawal, N. TransportTools: A Library for High-Throughput Analyses of Internal Voids in Biomolecules and Ligand Transport through Them. *Bioinformatics* **2022**, *38* (6), 1752–1753. https://doi.org/10.1093/bioinformatics/btab872.
(64) Tubiana, T.; Carvaillo, J.-C.; Boulard, Y.; Bressanelli, S. TTClust: A Versatile Molecular Simulation Trajectory Clustering Program with Graphical Summaries. *J. Chem. Inf. Model.* **2018**, *58* (11), 2178–2182. https://doi.org/10.1021/acs.jcim.8b00512.
(65) Roe, D. R.; Cheatham, T. E. I. PTRAJ and CPPTRAJ: Software for Processing and Analysis of Molecular Dynamics Trajectory Data. *J. Chem. Theory Comput.* **2013**, *9* (7), 3084–3095. https://doi.org/10.1021/ct400341p.
(66) Klvana, M.; Pavlova, M.; Koudelakova, T.; Chaloupkova, R.; Dvorak, P.; Prokop, Z.; Stsiapanava, A.; Kuty, M.; Kuta-Smatanova, I.; Dohnalek, J.; Kulhanek, P.; Wade, R. C.; Damborsky, J. Pathways and Mechanisms for Product Release in the Engineered Haloalkane Dehalogenases Explored Using Classical and Random Acceleration Molecular Dynamics Simulations. *J. Mol. Biol.* **2009**, *392* (5), 1339–1356. https://doi.org/10.1016/j.jmb.2009.06.076.
(67) Kaushik, S.; Marques, S. M.; Khirsariya, P.; Paruch, K.; Libichova, L.; Brezovsky, J.; Prokop, Z.; Chaloupkova, R.; Damborsky, J. Impact of the Access Tunnel Engineering on Catalysis Is Strictly Ligand-Specific. *FEBS J.* **2018**, *285* (8), 1456–1476. https://doi.org/10.1111/febs.14418.
(68) Schuetz, D. A.; de Witte, W. E. A.; Wong, Y. C.; Knasmueller, B.; Richter, L.; Kokh, D. B.; Sadiq, S. K.; Bosma, R.; Nederpelt, I.; Heitman, L. H.; Segala, E.; Amaral, M.; Guo, D.; Andres, D.; Georgi, V.; Stoddart, L. A.; Hill, S.; Cooke, R. M.; De Graaf, C.; Leurs, R.; Frech, M.; Wade, R. C.; de Lange, E. C. M.; IJzerman, A. P.; Müller-Fahrnow, A.; Ecker, G. F. Kinetics for Drug Discovery: An Industry-Driven Effort to Target Drug Residence Time. *Drug Discov. Today* **2017**, *22* (6), 896–911. https://doi.org/10.1016/j.drudis.2017.02.002.
(69) Copeland, R. A. The Drug–Target Residence Time Model: A 10-Year Retrospective. *Nat. Rev. Drug Discov.* **2016**, *15* (2), 87–95. https://doi.org/10.1038/nrd.2015.18.
(70) Sohraby, F.; Nunes-Alves, A. Advances in Computational Methods for Ligand Binding Kinetics. *Trends Biochem. Sci.* **2023**, *48* (5), 437–449. https://doi.org/10.1016/j.tibs.2022.11.003.